First-principles study of the electronic structures and magnetic properties of 3d transition metal-doped anatase TiO_2

2008 J. Phys.: Condens. Matter 20 125207

(http://iopscience.iop.org/0953-8984/20/12/125207)

J. Phys.: Condens. Matter **20** (2008) 125207 (6pp) doi:10.1088/0953-8984/20/12/125207

First-principles study of the electronic structures and magnetic properties of 3d transition metal-doped anatase TiO_2

Haowei Peng, Jingbo Li[1], Shu-Shen Li and Jian-Bai Xia

State Key Laboratory for Superlattices and Microstructures, Institute of Semiconductors, Chinese Academy of Sciences, PO Box 912, Beijing 100083, People's Republic of China

E-mail: jbli@semi.ac.cn

Received 18 December 2007
Published 25 February 2008
Online at stacks.iop.org/JPhysCM/20/125207

Abstract

We study the electronic structures and magnetic properties of the anatase TiO_2 doped with 3d transition metals (V, Cr, Mn, Fe, Co, Ni), using first-principles total energy calculations based on density functional theory (DFT). Using a molecular-orbital bonding model, the electronic structures of the doped anatase TiO_2 are well understood. A band coupling model based on d–d level repulsions between the dopant ions is proposed to understand the chemical trend of the magnetic ordering. Ferromagnetism is found to be stabilized in the V-, Cr-, and Co-doped samples if there are no other carrier native defects or dopants. The ferromagnetism in the Cr- and Co-doped samples may be weakened by the donor defects. In the Mn-, and Fe-doped samples, the ferromagnetism can be enhanced by the acceptor and donor defects, respectively.

1. Introduction

Practical application of spintronics requires room-temperature ferromagnetism (FM) in semiconductors [1]. Following the theoretical prediction that ZnO would become ferromagnetic with high transition temperature (T_C) by doping with 3d transition elements [2], intensive experimental and theoretical work has been done on dilute magnetic oxides including TiO_2 [3–12]. Several observations of room-temperature FM in Co- [3], Cr- [4] and V-doped [5] anatase TiO_2 have been reported. Meanwhile, a large number of theoretical studies have been done on the 3d transition metal (TM)-doped anatase TiO_2 (TiO_2:TM) [8–12]. In particular, TiO_2:Co has attracted much attention [8–10]. However, controversies still exist concerning the origin of the FM in these materials. Does the FM result from short-ranged superexchange interaction [8, 10], or a long-ranged carrier-mediated mechanism [13] or a double exchange like mechanism [8]? How do carriers introduced by the native defects and other impurities affect the magnetic properties [4, 6]? In order to elucidate the above questions, we systematically perform a series of calculations on V-, Cr-, Mn-, Fe-, Co- and Ni-doped anatase TiO_2.

On the other hand, the magnetic properties in GaAs:Mn and CdTe:Mn seem to be well understood. A band structure model, based on the p–d and d–d level repulsions between the Mn ions and host elements, has been successfully used to explained the magnetic ordering observed in all Mn-doped III–IV and II–VI semiconductors [14]. In this model, the holes play an important role in stabilizing the FM. In GaAs:Mn, the Mn d states strongly couple with the host valence p states, and the FM can be explained by the Zener model [15]. The FM in CdTe:Mn can be explained by double exchange, which is related to the d–d coupling between the Mn d states. However, there are no holes, so the antiferromagnetism (AFM) is stabilized, instead of the FM. According to this model, the FM in TiO_2:TM results from the double exchange interaction. In [11], the authors use a similar model, which they call the p–d hopping interaction, to explain the FM in TiO_2:Cr. For simplicity, the O_h (or T_d) local symmetry around the cation is used instead of the actual D_{2d} local symmetry in the anatase TiO_2. From this view, we would obtain FM in TiO_2:V and TiO_2:Fe just as in the case of TiO_2:Cr. However, the FM in TiO_2:Fe is claimed to be absent [7, 8], and the FM in TiO_2:V is claimed to result from the superexchange interaction [12]. In this paper, we calculate the electronic structures of TiO_2:TM. Due to the D_{2d} local symmetry around the dopants, the triple-degenerate t_2 state splits into a non-degenerate d_{xy} state and a double-degenerate d_{xz}/d_{yz} state. If the double-degenerate state is not fully occupied, the FM would be stabilized, and this is

[1] Author to whom any correspondence should be addressed.

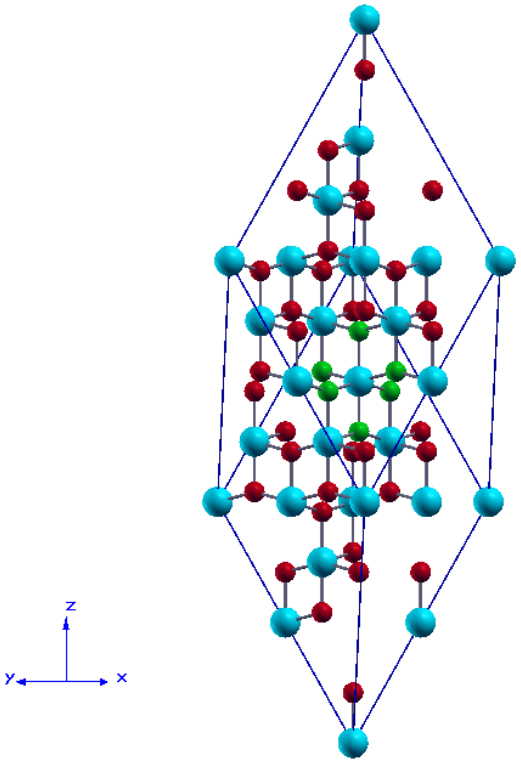

Figure 1. The 2 × 2 × 2 supercell of the anatase TiO_2. The big blue balls represent Ti atoms and the small red balls represent O atoms. The central six oxygen atoms represented with green balls form a distorted octahedron, based on which the coordinates (x, y, z) are defined.

(This figure is in colour only in the electronic version)

the origin of the FM in TiO_2:Cr and TiO_2:Co. In TiO_2:V, the hybridization between the non-degenerate V d_{xy} state and the host Ti d_{xy} state stabilizes the FM.

The rest of the paper is organized as follows. Section 2 briefly describes our calculation method. In section 3, first the chemical trend of the magnetic state stability is shown; second the electronic structure of the anatase TiO_2 without a dopant is presented; third the electronic structures of the V-, Cr-, Mn-, Fe-, Co- and Ni-doped anatase TiO_2 are discussed; finally a band coupling model is proposed to understand the chemical trend and the effects of the additional carrier defects or impurities. A brief summary of this paper is given in section 4.

2. Calculation methods

The calculations are performed with the local spin density approximation (LSDA) based on density functional theory (DFT), as implemented in the Vienna *ab initio* simulation package (VASP) [16]. The projector augmented wave method (PAW) [17] is chosen to represent the ionic potentials. A 48-atom 2 × 2 × 2 supercell is used in our calculations, as shown in figure 1. For the primitive unit cell, the LDA optimized lattice constants are tabulated in table 1; these agree very well with the experiment [18]. The calculated band gap is 1.9 eV, much smaller than the experiment, 3.2 eV [19], due to the well-known LDA underestimation. To model a defected system, the central Ti atom is replaced with a 3d TM atom (V, Cr, Mn, Fe, Co, Ni, respectively), yielding a dopant concentration of 6.25 at.%. To determine the magnetic ground state, the 48-atom supercells with two Ti atoms replaced are used, corresponding to a dopant concentration of 12.5 at.%. In the present calculations, we consider the configuration in which the two dopants are nearest neighbors. We also consider a uniformly distributed configuration; however, higher formation energies are needed, and the main physics is not changed. All the structures are relaxed until the Hellmann–Feynman force is less than 0.05 eV $Å^{-1}$, with the lattice constants fixed as the optimized ones. In all the total energy calculations, the cutoff energy of the plane-wave basis set is 400 eV, and a 6 × 6 × 6 Monkhorst–Pack k-grid [20] is used to sample the Brillouin zone of the supercell. The convergence of the total energy with respect to the cutoff and k-mesh is checked to be within 0.001 eV.

Table 1. The LDA optimized lattice constants of the anatase TiO_2, compared with the experimental results [18].

	a (Å)	c (Å)	u
Calculated	3.768	9.458	0.208(5)
Experiment	3.782	9.502	0.208

Table 2. The calculated total energy difference per dopant between antiferromagnetic and ferromagnetic states, $\Delta E = (E_{AFM} - E_{FM})/2$, and the magnetic moment per dopant (M) of the magnetic ground state.

Dopant	ΔE (meV)	M (μ_B)
V	75.5	0.79
Cr	174.5	1.85
Mn	−42.5	2.50
Fe	−0.5	1.69
Co	52.5	0.70
Ni	0.0	0.00

3. Results and discussion

3.1. Chemical trend of the magnetic state stability

In table 2, the calculated total energy differences per dopant between the antiferromagnetic and ferromagnetic states, $\Delta E = (E_{AFM} - E_{FM})/2$, are listed for the V-, Cr-, Mn-, Fe-, Co- and Ni-doped anatase TiO_2. The total energy difference indicates the stability of the ferromagnetic state. A positive total energy difference suggests that the ferromagnetic state is more stable than the antiferromagnetic state. The larger it is, the more the ferromagnetic state is stabilized. As shown in the table, TiO_2:V, TiO_2:Cr and TiO_2:Co are stabilized in the ferromagnetic state with high stability, which agrees with the experiments [3–5]. The previous calculations for TiO_2:Co [9] and TiO_2:V [12] also give similar results. TiO_2:Mn and TiO_2:Fe prefer the antiferromagnetic state, and TiO_2:Ni shows a paramagnetic behavior. From V to Ni, as the atomic numbers of the dopants increase, two maxima of the total energy

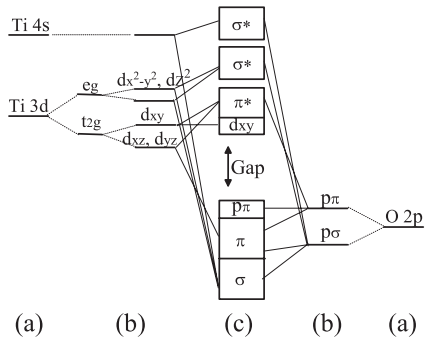

Figure 2. The molecular-orbital bonding diagram for pure anatase TiO_2: (a) atomic states, (b) crystal field split states, (c) final states. O p_σ and O p_π are the oxygen 2p states in and out of the Ti_3O plane, respectively.

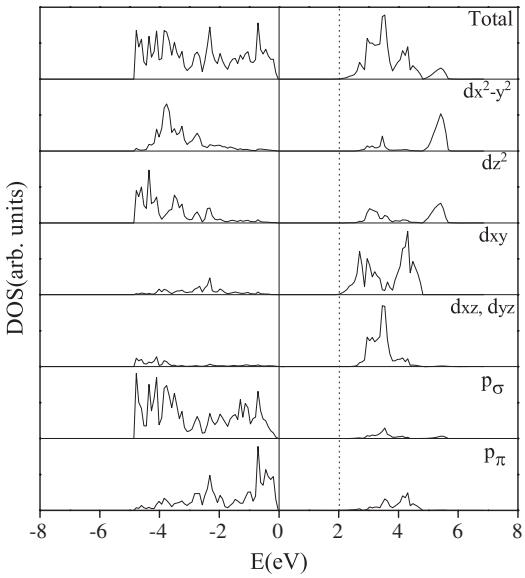

Figure 3. Total and projected densities of states (DOS) of the anatase TiO_2. The DOS is decomposed into Ti a_1 ($d_{x^2-y^2}$), Ti b_1 (d_{z^2}), Ti b_2 (d_{xy}), Ti e (d_{xz}/d_{yz}), O p_σ (in the Ti_3O plane) and O p_π (out of the Ti_3O plane) components. The top of the valance band (the vertical solid line) is taken as the zero of energy. The vertical dotted line indicates the conduction band minimum as a guide to the eye.

differences appear when Cr and Co are doped, respectively. Given that the T_C can be estimated qualitatively from the ΔE, high-T_C may be expected for TiO_2:Cr and TiO_2:Co if there are no native defects or other impurities. In the rest of this section, we will try to find out the physics behind this trend.

Table 2 also gives the magnetic moment per dopant of the magnetic ground state. As the atomic numbers of the dopants increase, the magnetic moment increases at first, and a maximum appears in the TiO_2:Mn, and then decreases to zero in the paramagnetic TiO_2:Ni. This trend will be explained in section 3.3.

3.2. Electronic structure of the undoped sample

Before studying the effects of the dopants, it is necessary to understand the electronic structure of the perfect anatase TiO_2 host.

Anatase TiO_2 crystallizes in a body centered tetragonal lattice, which is composed of distorted four-edge-shared octahedra, as shown in figure 1. The local symmetry around the cations is D_{2d}. According to crystal field theory, the five-fold degenerate Ti 3d state splits to a_1 ($d_{x^2-y^2}$), b_1 (d_{z^2}), b_2 (d_{xy}), and e (d_{xz}/d_{yz}) states; and the O 2p state can be decomposed into p_σ and p_π, which are in and out of the Ti_3O plane, respectively. A molecular-orbital bonding diagram is presented in figure 2, and is confirmed by the calculated density of states (DOS) shown in figure 3. The electronic structure of the perfect anatase TiO_2 is clearly illustrated by the two figures: the O p_σ states and the Ti $3d_{x^2-y^2}$, $3d_{z^2}$ states form the bonding σ states in the low energy region of the valence band, and the antibonding σ^* states in the high energy region of the conduction band; the middle energy regions of the valence and conduction bands are formed by the weak bonding between the O p_π states and the Ti $3d_{xz}$, $3d_{yz}$ states, as well as a small contribution from O p_σ and Ti $3d_{xy}$; the valence band maximum (VBM) consists of non-bonding O p_π states, and the conduction band minimum (CBM) consists of non-bonding Ti $3d_{xy}$ states.

Our results are in good agreement with previous FLAPW calculations [21]. In this paper we especially emphasize the D_{2d} local symmetry, because it is very important for understanding the magnetic properties of the doped samples as discussed in the followings.

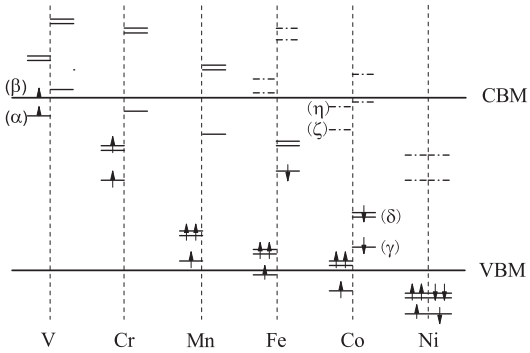

Figure 4. The calculated single particle electron energy states for the 3d TM dopants. The vertical dotted lines are used to separate the two spin channels. The single solid line is the d_{xy} state; the double solid lines are the double-degenerate d_{xz}/d_{yz} state; the dash–dot–dash lines are the $d_{x^2-y^2}$ state and the d_{z^2} state. Arrows with a tail stand for one electron, and arrows without a tail represent partial occupation of the states. The charge density contours of the states labeled (α) and (β) are shown in figure 5, and those of the states labeled (γ), (δ), (ζ), and (η) are shown in figure 6.

3.3. Electronic structures of the doped samples

When a Ti atom is replaced with a V, Cr, Mn, Fe, Co or Ni atom, a more negative ionic potential is introduced around the dopant site. As the atomic numbers of the dopants increase, the potential becomes lower and lower, and the states due to the dopants also shift to a lower energy. The trend is shown in figure 4, where we plot the calculated single particle electron energy states for the six 3d TM dopants.

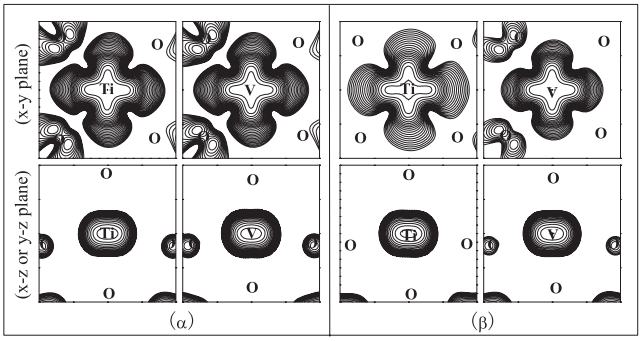

Figure 5. Charge densities in the Ti-centered and V-centered x–y and x–z (or y–z) planes for TiO_2:V: (α) the spin-up d_{xy} level due to the V dopant; (β) the spin-up CBM level which couples with the V $3d_{xy}$ level. The labels are defined in figure 4.

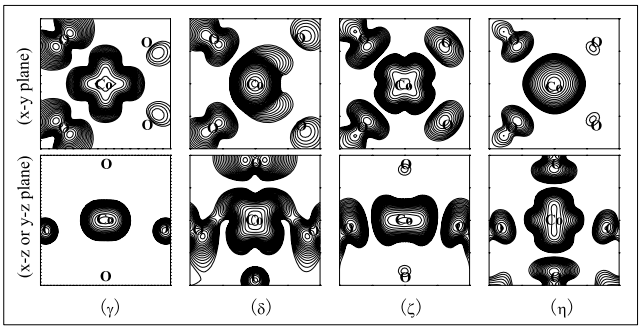

Figure 6. Charge densities in the Co-centered x–y and x–z (or y–z) planes for TiO_2:Co: (γ) the spin-down d_{xy} level; (δ) the spin-down double-degenerate d_{xz} and d_{yz} levels; (ζ) the spin-up $d_{x^2-y^2}$ level; (η) the spin-up d_{z^2} level. The labels are defined in figure 4.

To analyze the electronic structures of the doped samples, let us return to figure 2. If we replace the Ti 3d, and Ti 4s states with much lower Co 3d, and Co 4s states, and consider the spin splitting, we would obtain the single particle electron energy of the Co levels (coupling with the O p states) shown in figure 4, from the molecular-orbital bonding model. If we replace the Ti states with V states, similar analysis also works. However, because the V 3d states and Ti 3d states are very close, the V $3d_{xy}$ state couples with the Ti $3d_{xy}$ states which build up the host CBM, and the V $3d_{xy}$ state delocalizes a bit. As a result, in TiO_2:V the V $3d_{xy}$ and CBM levels are partially occupied. In figure 5, the charge densities of the two states (labeled (α) and (β) in figure 4) in TiO_2:V are shown, in both Ti-centered and V-centered planes. In this figure we see that charge density of the (β) state is very localized around the Ti atoms, which is characteristic of the host CBM as discussed in section 3.2. Meanwhile, as shown in the right-most patterns of the figure, there is also a considerable contribution from V dopant, which illustrates a strong coupling between the V $3d_{xy}$ and CBM Ti $3d_{xy}$ states. In figure 6, we show the charge densities of the four states (labeled (γ), (δ), (ζ), and (η) in figure 4) in TiO_2:Co. The charge density contour patterns illustrate that the four states have d_{xy}, d_{xz}/d_{yz}, $d_{x^2-y^2}$, and d_{z^2} characteristics, respectively. The π bonding between the Co-d_{xy}, Co-d_{xz}/d_{yz}, and O-p_π states, and the σ bonding between the Co-$d_{x^2-y^2}$, Co-d_{z^2}, and the O-p_σ states are also illustrated clearly. These patterns testify to the applicability of the molecular-orbital bonding model.

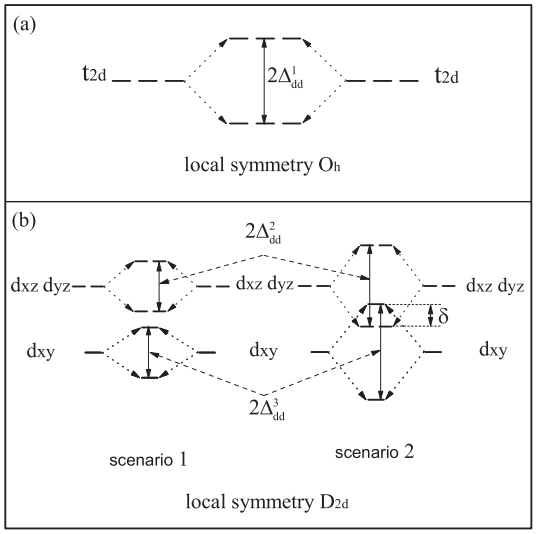

Figure 7. (a) The band coupling models for the O_h local symmetry materials. (b) Two scenarios for the D_{2d} local symmetry materials.

The electronic structures of the Cr-, Mn-, Fe-, Ni-doped samples can be analyzed as that of TiO_2:Co. As the atomic numbers of the dopants increase, more states are introduced into the band gap and under the VBM, and more states are occupied. From V to Mn, there are one, two, and three spin-up states occupied, corresponding to an increasing magnetic moment per dopant. And then, from Fe to Ni, the spin-down states begin to be occupied, and the net spin per dopant decreases. In TiO_2:Ni, the net spin is zero, leading to a paramagnetic property. This is the origin of the trend of the magnetic moment per dopant shown in table 2.

3.4. Band coupling model in D_{2d} local symmetry

In figure 7(a), the band coupling model in O_h or T_d local symmetry materials is shown, which successfully explains the magnetic ordering in ZnO:Mn and CdTe:Mn [14]. The two triple-degenerate t_{2d} (d_{xy}, d_{xz}, d_{yz}) states couple with each other, forming a bonding state and an antibonding state with a splitting $2\Delta^1_{dd}$. When a Mn atom replaces a Zn atom, the triple-degenerate t_{2d} state is occupied by three electrons. Then both the bonding and antibonding states are fully occupied, and the total energy of the system does not decrease via the ferromagnetic ordering so the FM is not stabilized in ZnO:Mn. The same happens for CdTe:Mn. However, if we introduce holes in the triple-degenerate t_{2d} state, via the ferromagnetic ordering, the total energy will decrease by $2m_h\Delta^1_{dd}$, where m_h is the number of holes in the triple-degenerate t_{2d} state, and the FM can be stabilized.

In anatase TiO_2, due to the D_{2d} local symmetry crystal field, the triple-degenerate t_{2d} state of the 3d dopants splits to a non-degenerate d_{xy} state and a double-degenerate d_{xz}/d_{yz} state. The splitting resulting from the coupling between the two double-degenerate d_{xz}/d_{yz} states is $2\Delta^2_{dd}$, and the splitting

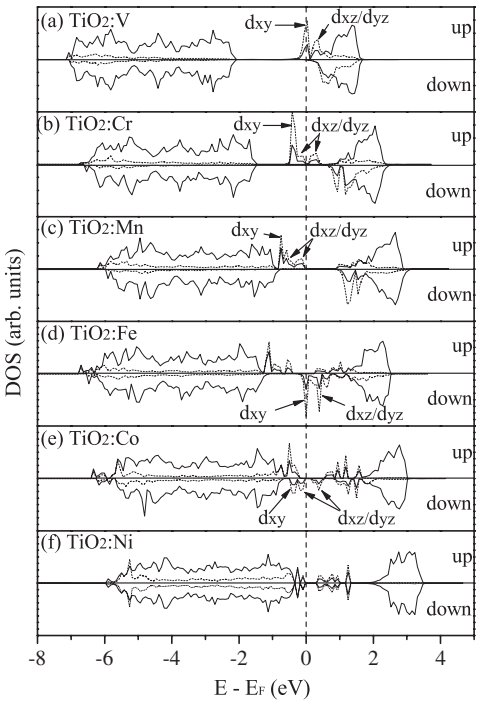

Figure 8. Total density of states per unit cell (solid line) and density of d states per TM atom projected on a TM site (dotted line) in (a) TiO_2:V, (b) TiO_2:Cr, (c) TiO_2:Mn, (d) TiO_2:Fe, (e) TiO_2:Co, and (f) TiO_2:Ni in the ferromagnetic configuration. The concentrations of the dopants is 12.5 at.%.

resulting from the coupling between the two non-degenerate d_{xy} states is $2\Delta_{dd}^3$. In figure 7(b), we show two possible scenarios: in the first scenario, the bonding and antibonding states of the d_{xy} states are separate from those of the d_{xz}/d_{yz} states; while in the second scenario, the bonding state of the d_{xz}/d_{yz} states is lower than the antibonding state of the d_{xy} states by δ. To prompt the crossing in the second scenario, the d states should be considerably delocalized via strong p–d coupling. However, in the anatase structure the d states couple with the O p_π states via weak π bonding, and the second scenario does not happen. In figure 8, the total density of states per unit cell and the density of d states per TM atom projected on a TM site for the ferromagnetic state are shown. In the figure, the peaks of the d_{xy} and d_{xz}/d_{yz} states near the Fermi level are marked out, confirming that the coupling is according to the first scenario. (Because the d_{xy} and d_{xz}/d_{yz} states are very delocalized in TiO_2:Ni, they are not marked out.) In TiO_2:Mn, all three d_{xy} and d_{xz}/d_{yz} states are occupied, so the total energy would not decrease via the ferromagnetic configuration, and the FM cannot be stabilized. In TiO_2:Cr and TiO_2:Co there is one hole in the double-degenerate d_{xz}/d_{yz} state, and the system will be more stable in the ferromagnetic state with a total energy decreasing by $2\Delta_{dd}^2$. In TiO_2:Fe, only the d_{xy} state is occupied, and according to the first scenario the FM would be wiped out, which is shown by our calculation and the experiments [6, 7]. If the crossing in the second scenario happens, via the ferromagnetic ordering, the total energy decreases by δ as shown in figure 7(b).

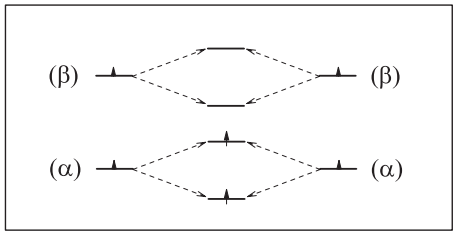

Figure 9. The band coupling model for TiO_2:V. (α) and (β) are the states defined in figure 4.

For TiO_2:V, the situation is more complicated due to the partially occupied characteristic of the electronic structure. If the electron occupies only the (α) state, the case would be the same as in TiO_2:Fe. Now we show the band coupling model for TiO_2:V in figure 9. Supposing the electron distribution is $(\alpha)^\kappa(\beta)^{1-\kappa}$ and the energy difference between the (α) state and the (β) state is ϵ, via the ferromagnetic ordering, the total energy of the TiO_2:V can decrease by $2(1-\kappa)\epsilon$, and the FM can be stabilized. Actually, the coupling model for TiO_2:V is very similar to the physical picture proposed by Coey *et al* that the hybridization between the 3d states of the magnetic dopants and other donor (e.g. an oxygen vacancy) states leads to the FM [13]. In V-doped anatase TiO_2, it is the hybridization between the host CBM states and the V dopant 3d state that stabilizes the FM.

All the discussions above are under the condition that no native defects or other impurities exist. However, the carrier (electron or hole) defects or impurities strongly affect the magnetic properties of TiO_2:TM. The band coupling model can give an intuitive explanation of their effects. For example, if the Cr dopants co-exist with half oxygen vacancies, the double-degenerate d_{xz}/d_{yz} state will be fully occupied due to the electrons from the oxygen vacancies, and the FM is wiped out. This effect has been confirmed by the experiment in [3], and a previous FLAPW calculation [11]. We perform a LSDA calculation on the system $Ti_{14}Mn_2O_{32}$ with two additional electrons, and a paramagnetic ground state is finally obtained as in TiO_2:Ni. We also perform another two numerical tests on two systems: $Ti_{14}Mn_2O_{32}$ with two additional holes, and $Ti_{14}Fe_2O_{32}$ with two additional electrons. Then, the double-degenerate d_{xz}/d_{yz} state will be half-occupied as in the case of TiO_2:Cr or TiO_2:Co, and the FM is stabilized. The calculated total energy differences per dopant for these two test systems are 77 and 163 meV, respectively. Perhaps the electrons from the oxygen vacancies are the trigger that strongly enhances the FM for Fe-doped samples post-annealed in a vacuum [6].

4. Summary

In this paper, the electronic structures of the 3d TM (V, Cr, Mn, Fe, Co and Ni)-doped anatase TiO_2 are calculated with a first-principles method. The D_{2d} local symmetry around the dopants is a key factor for understanding the electronic structures and the magnetic properties of the samples. A band coupling model, based on d–d level repulsions, is proposed and successfully explains the magnetic properties

in the various dopant cases. The hybridization between the host CBM states and the V dopant 3d state stabilizes the FM in the V-doped anatase TiO_2. The effects of the carrier defects and impurities are discussed. Without any other carrier defects or impurities, the V-, Cr-, and Co-doped anatase TiO_2 will be stabilized in a FM configuration. The donor defects and impurities will weaken the FM in Cr- and Co-doped anatase TiO_2. The FM in Mn- and Fe-doped anatase TiO_2 can be enhanced by the acceptor and donor defects, respectively.

Acknowledgments

J Li gratefully acknowledges financial support from the 'One-Hundred Talents Plan' of the Chinese Academy of Sciences. This work was supported by the National Natural Science Foundation of China under grant nos 60325416, 60521001, and 90301007.

References

[1] Wolf S A, Awschalom D D, Buhrman R A, Daughton J M, Von Molnár S, Roukes M L, Chtchelkanova A Y and Treger D M 2001 *Science* **294** 1488
[2] Dietl T, Ohno H, Matsukura F, Cibert J and Ferrand D 2000 *Science* **287** 1019
[3] Matsumoto Y, Murakami M, Shono T, Hasegawa T, Fukumura T, Kawasaki M, Ahmet P, Chikyow T, Koshihara S and Koinuma H 2001 *Science* **291** 854
[4] Kaspar T C, Heald S M, Wang C M, Bryan J D, Droubay T, Shutthanandan V, Thevuthasan S, McCready D E, Kellock A J, Gamelin D R and Chambers S A 2005 *Phys. Rev. Lett.* **95** 217203
[5] Hong N H, Sakai J and Hassini A 2004 *Appl. Phys. Lett.* **84** 2602
[6] Lee H M and Kim C S 2007 *J. Magn. Magn. Mater.* **310** 2009
[7] Balcells Ll, Frontera C, Sandiumenge F, Roig A, Martínez B, Kouam J and Monty C 2006 *Appl. Phys. Lett.* **89** 122501
[8] Park M S, Kwon S K and Min B I 2002 *Phys. Rev.* B **65** 161201(R)
[9] Yang Z, Liu G and Wu R 2003 *Phys. Rev.* B **67** 060402(R)
[10] Janisch R and Spaldin N A 2006 *Phys. Rev.* B **73** 035201
[11] Ye L-H and Freeman A J 2006 *Phys. Rev.* B **73** 081304(R)
[12] Du X, Li Q, Su H and Yang J 2006 *Phys. Rev.* B **74** 233201
[13] Coey J M D, Venkatesan M and Fitzgerald C B 2005 *Nat. Mater.* **4** 173
[14] Dalpian G M *et al* 2006 *Solid State Commun.* **138** 353
[15] Dietl T, Haury A and Merle d'Aubigné Y 1997 *Phys. Rev.* B **55** R3347
[16] Kresse G and Joubert D 1996 *Comput. Mater. Sci.* **6** 15
[17] Kresse G and Joubert J 1999 *Phys. Rev.* B **59** 1758
[18] Burdet J K, Hughbanks T, Miller G J Jr and Smith J V 1987 *J. Am. Chem. Soc.* **109** 3639
[19] Tang H, Berger H, Schmid P E, Lévy F and Burri G 1997 *Solid State Commun.* **23** 161
[20] Monkhorst H J and Pack J D 1976 *Phys. Rev.* B **13** 5188
[21] Asahi R, Taga Y, Mannstadt W and Freeman A J 2000 *Phys. Rev.* B **61** 7459